3D spatial resolution evaluation for helical CT according to ASTM E1695 – 95

Jakub Laznovsky[1], Adam Brinek[1], Jakub Salplachta[1], Tomas Zikmund[1], Ben Young[2], Zuzana Patakova[2], Jozef Kaiser[1]

CEITEC CTLAB

[1]CEITEC - Central European Institute of Technology, Brno University of Technology, Czech Republic

Thermo Fisher SCIENTIFIC

[2]Thermo Fisher Scientific Inc., Vlastimila Pecha 12, Brno, Czech Republic

Abstract

Knowledge of valid spatial resolution is essential for quantitative analysis using X-ray computed tomography. Due to the spatial resolution, it is possible to determine with what detectability the imaging system can measure an internal structure. Based on the spatial resolution knowledge, the smallest object size that can be distinguished in resulting images can be determined. Each component in the imaging system affects the value of spatial resolution, and the final value is defined as a product of all comprised components. In this paper, spatial resolution according to standard ASTM E1695 – 95 was calculated. This standard uses edge response function (ERF), point spread function (PSF) to modulation transfer function (MTF) approach for the calculation of spatial resolution in each plane. For the calculation was used a sphere phantom, which is convenient for the study of spatial resolution in all three orthogonal planes. Final 3D spatial resolution was evaluated as a mean of particular spatial resolutions in individual orthogonal cutting planes.

I Materials and methods

Designed phantom

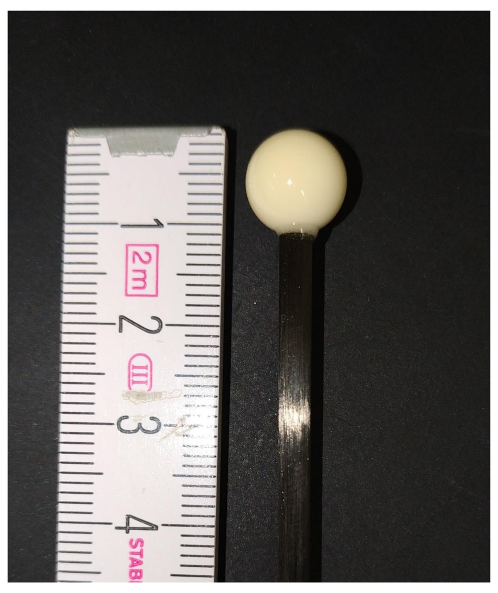

Fig. 7: Designed ball phantom

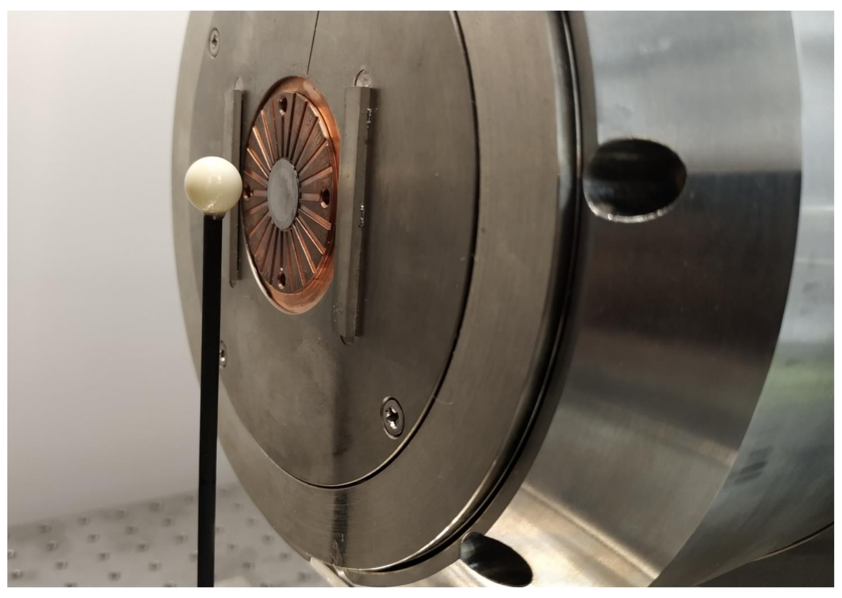

Fig. 8: Acquisition of the ball phantom

Acquisition

Table 1: Acquisition parameters for both: circular and Space-Filling measurement

Parameter:	Circular	Space-Filling
Voxel size	2.3 µm	2.3 µm
Voltage	100 kV	100 kV
Current	160 µA	160 µA
Exposure time	0.6 s	0.6 s
Projections	2880	2880
Filter	0.22 mm stainless steel	0.22 mm stainless steel
Reconstruction	Filtered back projection	Iterative reconstruction

Phantom measurement in Space filling trajectory

Ball phantom was designed for determination of spatial resolution. The material type comply mentioned ASTM standard suitable for this study. The ceramic ball is manufactured with high precision and minimal surface roughness (Grade 25). The phantom consist of a ball glued to a carbon bar. Despite [1] indicate that the rod should be used, the ball phantom is more promising when the 3D resolution should be achieved. The rod enables the analysis only in the parallel cross section to the beam. The ball phantom was chosen for the reason that the orthogonal cross sections can be easily achieved. For the calculation itself, three slices were chosen in every plane (transversal, coronal, sagittal) approximately crossing the middle of the ball.

The phantom was scanned on Heliscan MK1, the product of Thermo Fisher Scientific. Two scans of the phantom were executed. One measurement of the phantom with Space filling trajectory [2], [3] and one measurement of the phantom with circular trajectory. Both measurements were performed with the same parameters.

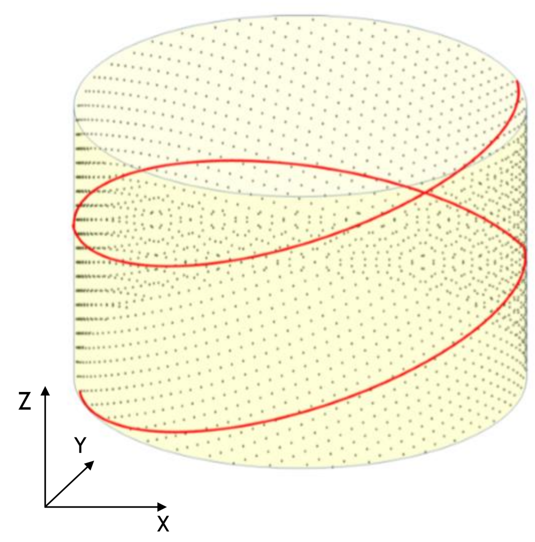

Fig. 1: Space filling trajectory scheme. Red line – Helical scan, Dark dotes – Space-Filling scan

The circular trajectory has advantages in the scanning of the samples with similar sizes in all directions. The helical trajectory is convenient in the case of scanning long sample exceeding the detector size. There is no need of stitching individual scans which can cause grey value inhomogeneity within one material, and the scanning time is shortened. Another significant advantage is the quality of the top sample surface which can be used for correlation with other imaging techniques.

Benefits of Space-Filling trajectory

- High cone-angle imaging
- Entire detector area is fully utilized
- Half the overscan required in comparison with Double-Helix scan
- More uniform sampling of the sample – reduction of artifacts

II Procedure

Data processing

Phantom material detection by Hough transform. See fig. 2 → Extraction of all pixels corresponding to the bordered area. See fig. 2, fig. 3 → Segregation of individual pixels into bins. See fig. 4 → PSF obtained as analytical derivative of cubic fit applied to smoothed ERF. See fig. 5 → Resulting MTF calculated as Fourier Transform of PSF See fig. 6

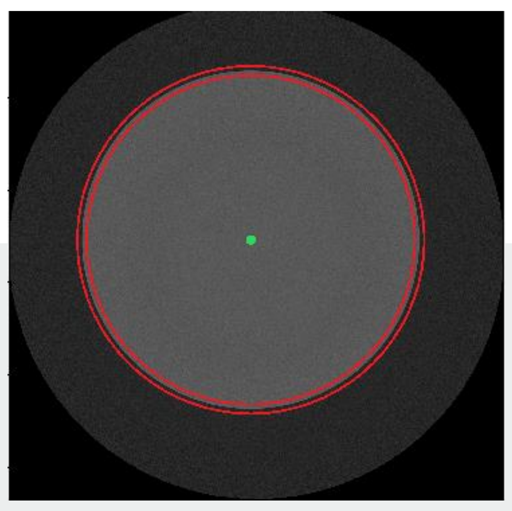

Fig. 2: Measured ball phantom depicted in xy plane. Green point – the estimated center of mass. The area enclosed by two red circles enters the calculation process

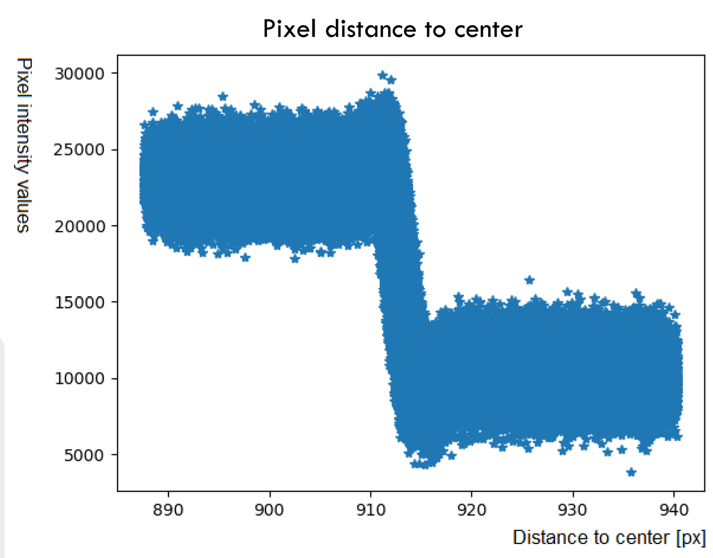

Fig. 3: Extracted pixels in the dependence to center of mass

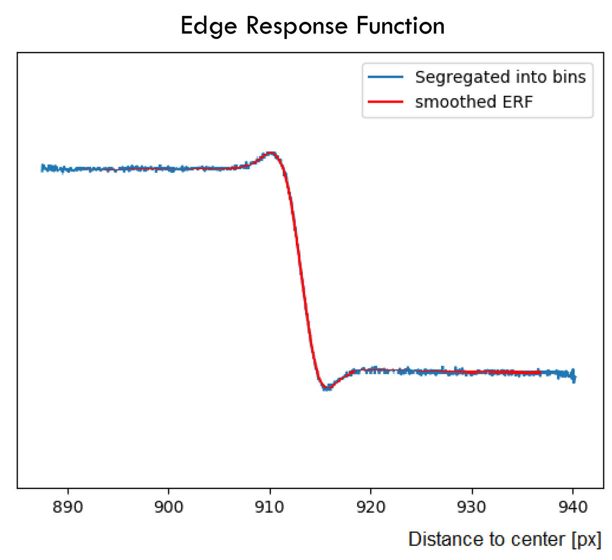

Fig. 4: Edge Response Function segregated into bins (blue line) and smoothed (red line)

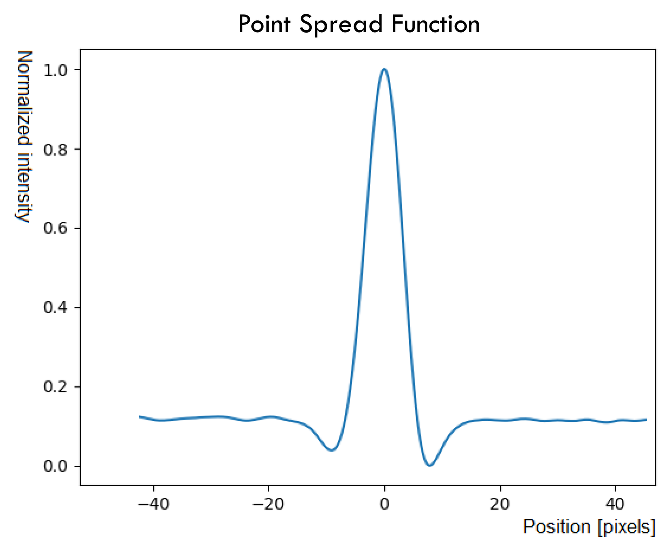

Fig. 5: Normalized Point Spread Function

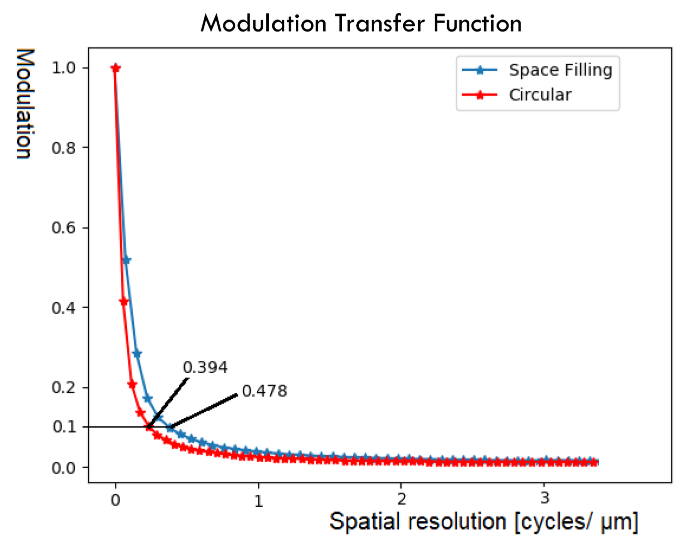

Fig. 6: Resulting Modulation Transfer Function of Circular (red line) and Space-Filling (blue line) trajectory

Results

Table 5: Results of the spatial resolution in 10 % of MTF

Measurement:	Circular	Space-Filling
XY plane	2.536 µm	2.090 µm
XZ plane	6.110 µm	5.531 µm
YZ plane	5.456 µm	4.498 µm
3D	4.701 µm	4.039 µm

In general, the main difference in the results is between the parallel and perpendicular planes with the X-rays. This fact can be explained that the cone beam can cause a nonlinear magnitude of the sample in different cross-sections. Also, the reconstruction algorithm is using the AutoFocus function, which affects the sharpness of the images [3].

The better spatial resolution of Space-Filling trajectory is provided due to cone beam artifacts reduction and more uniform sampling of the data. The final 3D spatial resolution of the system for the scan with circular and helical trajectory are 4.701 µm ± 0.235 and 4.039 µm ± 0.202, respectively. The spatial resolution results are in the magnitude of the voxel size. The uncertainty is 5% according to the standard [3].

3D resolution

The main focus of this paper is in the method for achieving the 3D spatial resolution. The method is following the ASTM E1695 – 95 [1]. According to this standard, spatial resolution calculation is based on the quantitative measurement of the Modulation Transfer Function (MTF). MTF relates on the spatial frequency of sample features and the corresponding loss of contrast in the image. In this study, 3D spatial resolution is considered as a particular spatial resolution in individual orthogonal cutting planes. Thanks to this approach, we can observe and compare the dependence of the sample placement in the system to the spatial resolution.

III Conclusion

The phantom consisting of carbon stick and the ceramic ball was designed based on ASTM E1695 – 95. CT measurements of the phantom with Space Filling and circular trajectory were performed. From every dataset, three slices corresponding to individual three cutting planes were chosen. Corresponding MTFs and appropriate spatial resolutions were calculated based on these three slices. All calculations were done in Python programming environment. The value of 3D spatial resolution was computed as an average of spatial resolutions in all three planes for the corresponding dataset. The resulting spatial resolution of the scan with circular and helical trajectory are 4.701 µm ± 0.235 and 4.039 µm ± 0.202, respectively.

CEITEC – Central European Institute of Technology
Brno University of Technolgy, Purykňova 123
612 00 Brno, Czech Republic
www.ceitec.eu

Jakub Laznovsky
Laboratory of X-ray Micro and Nano CT
e-mail: jakub.laznovsky@ceitec.vutbr.cz
phone: +420 541 149 867
web: www.ctlab.ceitec.eu

REFERENCES

[1] Standard Test Method for Measurement of Computed Tomography (CT) System Performance: E 1695 – 95. 1st edition. United States: American Society for Testing and Materials, 2013

[2] A. M. Kingston, G. R. Myers, S. J. Latham, B. Recur, H. Li, A. P. Sheppard. Space-Filling X-Ray Source Trajectories for Efficient Scanning in Large-Angle Cone-Beam Computed Tomography. IEEE Transactions on Computational Imaging [online]. 2018, 4(3), 447-458. DOI: 10.1109/TCI.2018.2841202. ISSN 2333-9403.

[3] T. Varslot, A. Kngston, G. Myers, A. Sheppard. High-resolution helical cone-beam micro-CT with theoretically-exact reconstruction from experimental data. Medical Physics [online]. 2011, 38(10), 5459-5476. DOI: 10.1118/1.3633900. ISSN 00942405.

ACKNOWLEDGMENTS

This research was carried out with financial support TA ČR (project TN01000008) and under the project CEITEC 2020 (LQ1601) with financial support from the Ministry of Education, Youth and Sports of the Czech Republic under the National Sustainability Programme II and support of CEITEC Nano Research Infrastructure (MEYS CR, 2016–2019).

CEITEC BRNO UNIVERSITY OF TECHNOLOGY